SEAKEEPING PREDICTION OF DEEP-V HIGH SPEED CATAMARAN USING COMPUTATIONAL FLUID DYNAMICS APPROACH

Ahmad Fitriadhy, Nur Amira Adam, N. Amalina, S. A. Azmi
Program of Maritime Technology, School of Ocean Engineering, Unversiti Malaysia Terengganu,
21030 Kuala Terengganu, Terengganu, Malaysia
Email: naoe.afit@gmail.com; amiraadam.nur@gmail.com; amalina@gmail.com; s.azmi@gmail.com

Abstract -- *Seakeeping is the dynamic response of the ship in waves that may affect to passenger's uncomfortability due to a harsh environmental condition. Therefore, an extensive assessment of seakeeping performance in the initial step of ship design is necessarily required. The authors here proposed to analyze the seakeeping performance of 'deep-V' high speed catamaran using Computational Fluid Dynamics (CFD) approach. Several effects of Froude number (Fr), wave-length (λ/L) and wave height (Hw/L) was considered to predict the RAO of heave and pitch motions. The results showed that the heave and pitch motions were inversely proportional to the Fr in the range of Fr 0.5 to 1.0. In shorter wavelength (λ<0.75), RAO of the heave and pitch motions were insignificant. However, the heave and pitch motions increase of wavelength (λ>0.75) was proportional with the increased RAO of the heave and pitch motions. The further increase of wavelength (λ>1.75) resulted in less RAO of the heave and pitch motions. The increase in wave height from 0.0257 to 0.0375 was affected by the RAO of the heave and pitch motions and her seakeeping performance. The prediction results in term regular sea state, showed the preliminary data very useful to predict the optimal condition that reduces the amplitude of motion.*

Keywords: *Deep-V Catamaran; CFD; RAO; Heave; Pitch*

INTRODUCTION

Multi-hull ship have been earned attention among the naval architecture because of their advantages compared to the monohull ship, such as the ability to provide lower draught, excellent seakeeping performance, better transverse stability and wider deck area (Gunawan, Kurniawan, & Jamaluddin, 2015), (Luhulima, Setyawan, & Utama, 2014), (Sun et al., 2016) and (Setyawan, Utama, Murdijanto, Sugiarso, & Jamaluddin, 2010). However, according to the study from Vakilabadi et al. (Vakilabadi, Khedmati, & Seif, 2014), the quantities of the ship motion such as heave and pitch motions also an important element to consider for the operability of the crew and equipment. Therefore, the seakeeping performance of multi-hull ship is a very prominent aspect to be analyze in the early design stage to ensure safe ship motion in a regular wave condition.

There is a number of ways to estimating the seakeeping behavior of ships. Several researchers had studied the behavior of multihull ship using analytical, experimental and numerical methods to predictions the seakeeping performance. According to (Grande & Xia, 2002), (Belknap, 2008), (Lin et al., 2017) and (Aribenchi, 2017) seakeeping performance was also predicted using strip theory method. Besides that, (Vakilabadi, Khedmati, & Seif, 2014),

(Yanuar, Ibadurrahman, Karim, & Ichsan, 2017), (Abdul Ghani & Wilson, 2017) and (Zotti, 2007) studies the behavior of catamaran ship using experimental method approach that have their own disadvantages such as complex procedure, costly and time-consuming. In the other ways, numerical method using Computational Fluid Dynamics (CFD) also offers more easer procedure and accurate data to study hydrodynamics characteristics of 'deep-V' catamaran. The validation of CFD result also was proven by comparing with experimental data (Haase et al., 2016), (Iglesias, Zamora, Fernández, & Pavón, 2006), (Salas et.al., 2004) and (Swidan, 2016).

This paper presents a Computational Fluid Dynamics (CFD) simulation approach to analyses seakeeping performance of a 'deep-V' catamaran ship in head-seas regular wave. Here a commercial CFD software, namely Numeca Fine™/Marine v3.1-1, is utilized by applying the incompressible unsteady Reynolds Average Narvier Strokes Equation (RANSE). This RANSE and continuity equation are discretized by the finite volume method based on Volume of Fluid (VOF) to deal with the non-linear free surface. In addition, the computational domain with adequate numbers of grid meshes of the 'deep-V' catamaran ship was carefully determined before simulations. Basically, this is solved by means of

a mesh independent study to estimate the optimal domain discretization. In this computational simulation, the small-scale geometry model was tested in several parameters, such as effect of Froude numbers (Fr), wavelengths (λ/L) and wave heights (Hw/L) are considered. The seakeeping performance of 'deep-V' catamaran was presented in Response Amplitude Operator (RAO) and visualization.

CFD MODELLING
Conservation Equation
The flow solver can deal with multi-phase flows and moving grids. In the multi-phase continuum, considering incompressible flow of viscous fluid under isothermal conditions, mass, momentum and volume fraction conservation equations can be expressed (by using the generalized form of Gauss' theorem) as:

$$\frac{\partial}{\partial_t} \int_S \rho \left(\vec{U} - \vec{U}_d \right) . \vec{n} \, dS = 0 \tag{1}$$

$$\frac{\partial}{\partial_t} \int_V \rho U_i dV + \int_S \rho U_i \left(\vec{U} - \vec{U}_d \right) . \vec{n} \, dS = \int_S \left(\tau_{ij} I_j - p I_i \right) . \vec{n} \, dS + \int_V \rho g_i \, dV \tag{2}$$

$$\frac{\partial}{\partial_t} \int_V c_i dV + c_i \left(\vec{U} - \vec{U}_d \right) . \vec{n} \, dS = 0 \tag{3}$$

where V is the control volume, bounded by the closed surface S with a unit normal vector $\vec{n}$ directed outward that moves at the velocity $\vec{U}_d$ with a unit normal vector $\vec{n}$. The notation of $\vec{U}$ and p represent the velocity and pressure fields, respectively. τ_{ij} and g_i define the components of the viscous stress tensor and the gravity vector, respectively; whereas I_j is a vector whose components vanish, except for the component j which is equal to unity. c_i is the ith volume fraction for fluid i and is used to distinguish the presence ($c_i = 1$) or the absence ($c_i = 0$) of ith fluid. Since a volume fraction between 0 and 1 indicates the presence of a mixture, the value of 1/2 is selected as a definition of the interface.

Turbulence model
In the case of a basic computation for turbulent condition, we propose the SST k −ω (SST for shear-stress transport) model, which is available inside ISIS-CFD solver code, where k is the turbulent kinetic energy and ω is the specific dissipation rate.

It also should be noted here that when calculating turbulence quantities, it is important to consider an appropriate cell meshing size. This can be explained by the fact that during computations using the Navier-Stokes equations the boundary layer near a solid wall contains high gradients. To properly capture it a sufficient

number of grid points inside the boundary layer is essential. Here, an appropriate estimation of the cell meshing size y_{wall} for Navier-Stokes simulations including turbulence depends on the local Reynolds number, which is computed based on the wall variable y⁺ This is a y⁺ dimensionless parameter representing local Reynolds number in the near wall region. Referring to Numeca (2013), the value of y⁺ value associated with the first node near the wall will be referred to as y_1^+, where the equation of y_1^+ can be written as:

$$y_1^+ = \frac{\rho u_\tau y_{wall}}{\mu} \tag{4}$$

where u_τ is the friction velocity,

$$u_\tau = \sqrt{\frac{\tau_{wall}}{\rho}} = \sqrt{\frac{1}{2}\rho (V_{ref})^2 C_f} \tag{5}$$

Heave and Pitch Motion
The degree of freedom (D.O.F) represented the possible translations and rotation of the body. The heaving and pitching motion noted as translation and rotation respectively along X, Y, and Z-axis that define the behavior of the monoricat under sailing. The coupled equation of heave and pitch motions are solved in the time domain for regular waves. These equations are demonstrated as follows:

$$(M + A_{33}) \frac{d^2\eta_3}{dt^2} + B_{33}\frac{d\eta_3}{dt} + C_{33}\eta_3 + A_{35}\frac{d^2\eta_5}{dt^2} + B_{35}\frac{d\eta_5}{dt} + C_{35}\eta_5 = F_3 \tag{6}$$

$$A_{53}\frac{d^2\eta_3}{dt^2} + B_{53}\frac{d\eta_3}{dt} + C_{53}\eta_3 + (I_{55}+A_{35})\frac{d^2\eta_5}{dt^2} + B_{35}\frac{d\eta_5}{dt} + C_{55}\eta_5 = F_5 \tag{7}$$

In these equations, M is the vessel mass, I55 is the moment of inertia in pitch and A_{ij}, B_{ij} and C_{ij} are coefficients of added mass, damping and restoring coefficient respectively. Also, F_3 and F_5 are vertical force and longitudinal subverting moment on the vessel respectively [17].

Table 1. Principle dimensions of "deep-V" catamaran ship.

Description	Demi-hull	Catamaran
Length between perpendicular, *LBP (m)*	1.740	1.740
Breadth, *B (m)*	0.678	0.678
Draft, *T (m)*	0.080	0.080
Wetted surface area, *WSA (m²)*	0.256	0.512
Volume of displacement, ∇ *(m³)*	0.0082	0.027
Displacement, *Δ (tonnes)*	7.222	10.792

Computation Domain and Mesh Generation

The computational domain of the catamaran model associated with the unstructured hexahedral meshes is shown in Fig. 3. An extra local refinement of the mesh was added around the free surface to capture the waves that are generated by the catamaran hull during computation. In addition, the local box refinement was employed surrounding the global meshed computational domain. Correspondingly, the maximum number of this local box refinement was set as the same as the maximum global
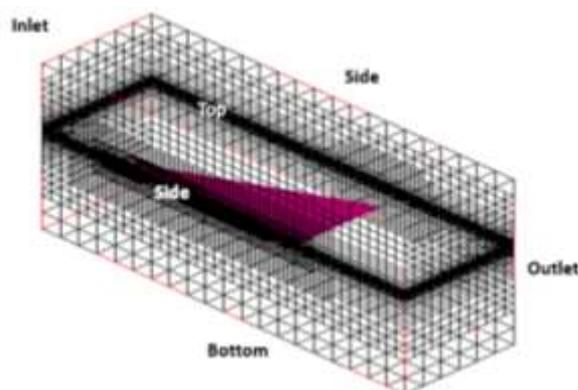

Figure 2. Boundary condition of a high-speed "deep-V"catamaran model.

Referring to Table 3, the external (EXT) boundary type condition was assigned to treat velocity and pressure condition. In addition, the boundary condition for the top and bottom of the

SIMULATION CONDITION
Ship Particular

In the computational simulation, the principle dimension of the 'deep-V' catamaran composed of two demi-hulls is clearly presented in Table 1.

Figure 1. 3D model of high speed "deep-V" catamaran model.

number of refinements. In this simulation, the local maximum number was determined as equal to 12. Meanwhile, another surface was employed as a triangle purposed to capture the effective area in both x and y directions, where the Kelvin waves will appear. Furthermore, the effective domains for the CFD simulation in deep water conditions or infinite water depth. Considering on less computational time, the authors apply the symmetrical computational domain model (demihull).

Table 2. Computation domain and boundary setting condition.

Description	Distance with respect to origin point	Type	Condition
Xmin (Inlet)	1.0 L_{mh}	EXT	Far Field
Xmax (Outlet)	3.0 L_{mh}	EXT	Far Field
Zmin (Bottom)	1.5 L_{mh}	EXT	Prescribed pressure
Zmax (Top)	0.5 L_{mh}	EXT	Prescribed pressure
Ymin (Side)	1.5 L_{mh}	EXT	Far Field
Ymax (Side)	1.5 L_{mh}	EXT	Far Field

patches domain were assigned as 'prescribed pressure'. In this mode, the pressure was imposed during the computation initialization, where the updated hydrostatics pressure was

then applied. This means that the pressure is not constantly at 0 (zero) during the computational but it dynamically updates due to the cell mesh moving vertically towards the free surface position. Since this computational will run in the presence of wave, the inlet path will be assigned as 'wave generator' that available for regular and irregular condition. The values for the wave condition will be computed by using tool names 'waves generation info'. Concerning the boundary condition for the 'deep-V' catamaran ship, surfaces were assigned as solid patched, where a wall-function condition was employed to these surfaces.

Table 3. Mesh Independent study on symmetrical catamaran.

Case	Initial Number of Meshing	Total Number of cells in initial mesh	Number of Cell Meshing	Heave motion (m)	Pitch motion (^{0})
A	5 x 4 x2	40	823779	0.005483	1.026354
B	6 x 5 x 3	90	1121405	0.005264	1.351600
C	7 x 5 x 2	170	2055700	0.007321	1.416003
D	20 x 6 x 2	240	2649747	0.007310	1.396540

For the current CFD simulation, the mesh independent study of catamaran was conducted to assess a proper total number of cell meshing for the whole simulations. The results of the mesh independent study are summarised in Table 4 (S/L = 0.4 and Fr = 0.8). The meshing generation of catamaran model for the main hull block and outriggers surface is created in HEXPRESS v3.3.1. It should be noted that adequate mesh number is important to maintain numerical accuracy and steadiness in computation result, regardless of the longer CPU time. Hence, a mesh independent study is necessary to examine each of three cell meshing initial number. Table 4 refers to the mesh independent study result. The initial cell meshing of 170 in case C is selected from all the cases because it has reasonable accuracy of CFD solution. This can be explained by the fact that the increase of initial cell meshing number to 240 in computation was unnecessary due to insignificant influence on the computational result for total resistance.
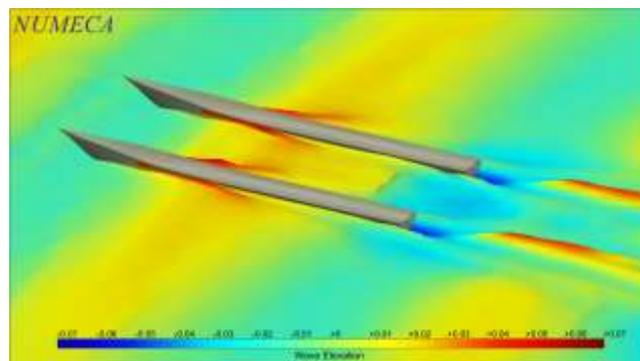
(a)
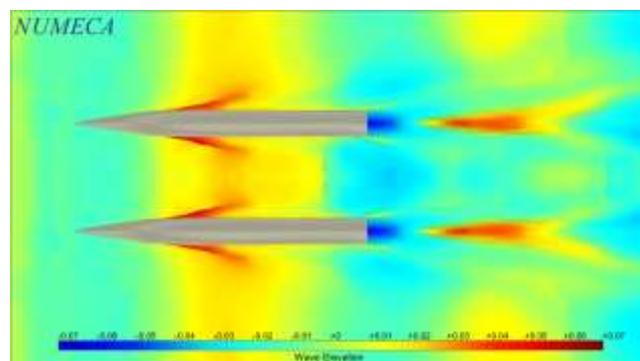
(b)

Figure 3. CFD visualization (a) perspective view, (b) plan view, where Fr= 0.8, S/L=0.2, λ/L=1.0, Hw/L=0.027 and Θ= 0°

RESULT AND DISCUSSION

Referring to Table 5, 6 and 7, the seakeeping simulations of the 'deep-V' catamaran model has been successfully carried using Computational Fluid Dynamic Approach. The results are then presented in the form of her response amplitude operator (RAO) of heave and pitch motions. Here, the seakeeping investigation of the 'deep-V' catamaran model has been in a typical regular wave with wavelength and wave height within the range of 0.25 to 3.00 and 0.0257 to 0.0375, respectively.

Effect of Froude number (Fr)

Referring to Fig. 4, subsequent increase from Froude number 0.5 up to 1.1 was decrease the heave and pitch motion. It should be noted that the heave motion of 'deep-V' catamaran decreased from 0.02552 m to 0.001181 m as Fr=0.5 to 1.1. Although, the pitch motion decreases from 3.851286 º to 0.622232 º. The result also showed that the higher the Froude number, the more the slope of the post-peak descending region will be and the lower of Froude number was prone to down degrade the seakeeping performance of the 'deep-V' catamaran due to the higher response of heave and pitch motion (Fitriadhy, Razali, & AqilahMansor, 2017) and (Vakilabadi et al., 2014).
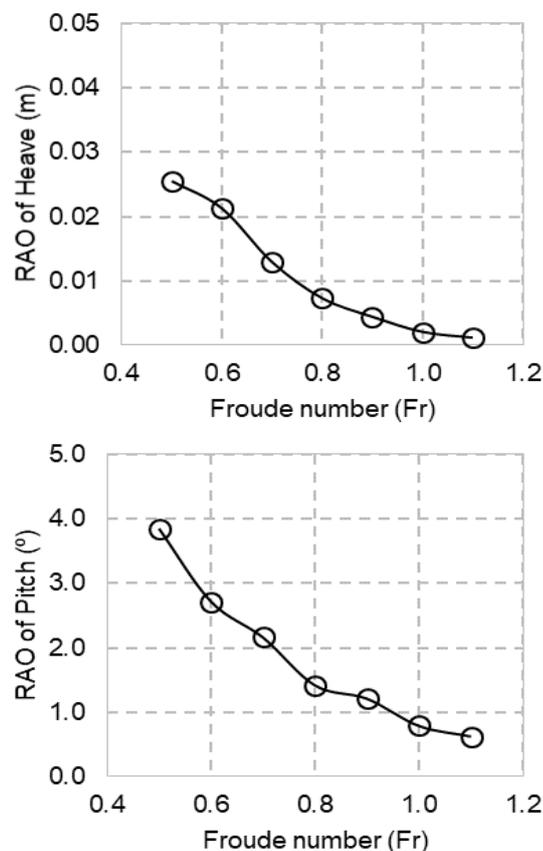

Figure 4. Heave and pitch motions for 'deep-V' catamaran ship at various Froude number, $\lambda/L= 1$, Hw=/L=0.02586, $\Theta=0^0$.

Table 4. Heave and pitch movement for 'deep-V' catamaran at various Froude number (Fr).
Froude Number (Fr), $\lambda/L= 1$, Hw/L = 0.0257 and $\Theta = 0^o$.

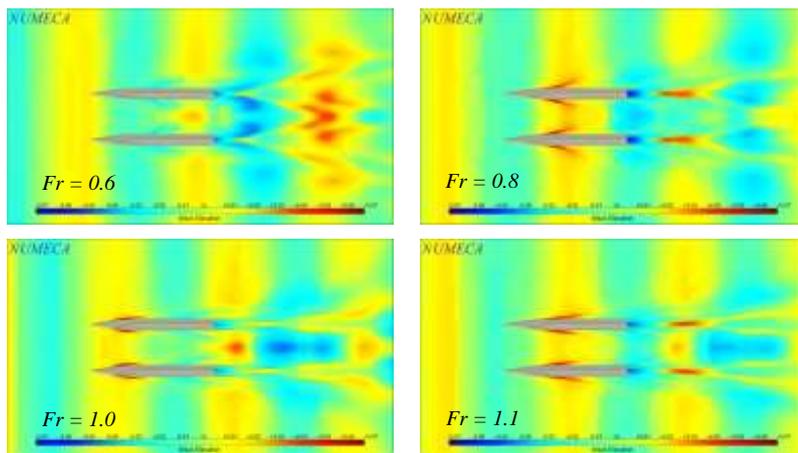| Froude Number (Fr)	$\lambda/L= 1$, $H_W/L= 0.0257$ and $\Theta = 0^o$	
	Heave Motion (m)	Pitch Motion (°)
0.5	0.02552	3.851286
0.6	0.021287	2.716644
0.7	0.012938	2.159949
0.8	0.007321	1.416003
0.9	0.004418	1.208340
1.0	0.002073	0.786671
1.1	0.001181	0.622232

Figure 5. Free surface elevation for 'deep-V' catamaran ship, λ/L= 1, Hw/L=0.02586, Θ=0°.

Effect of Wavelength (λ/L)

The RAO characteristics of the heave and pitch motions were displayed in Fig. 6, where the details result a completely presented in Table 5. In this figure, the graph show that the heave motion were relatively steady at λ/L= 0.25 and λ/L= 0.5. The heave motion then increases slightly at λ/L= 0.75 and 1.0. The continuously increase of wavelength from λ/L= 1.0 until 1.75 will increase the heave motion until reach a highest point at λ/L= 1.00. The increase of wavelength from λ/L= 1.75 to 3.00 has been decline gradually the heave motion until the motion steady again. In additional, the graph also shows the pitch motion of the 'deep-V' catamaran low at λ/L= 0.25 up to 0.75. It should have noticed that the pitch motion of the 'deep-V' catamaran model significantly increased from 0.081o to 0.043o as wavelength increase λ/L= 0.75 to 1.75. The pitch motion for wavelength λ/L=1.75 to 3.00 decrease from 2.76° to 1.91°.

The critical point of the heave and pitch motion is at λ= 1.75 with 0.042524 m and 2.76° respectively. The critical point at heave and pitch motion describe the dangerous condition to the 'deep-V' catamaran (Castiglione & Bova).
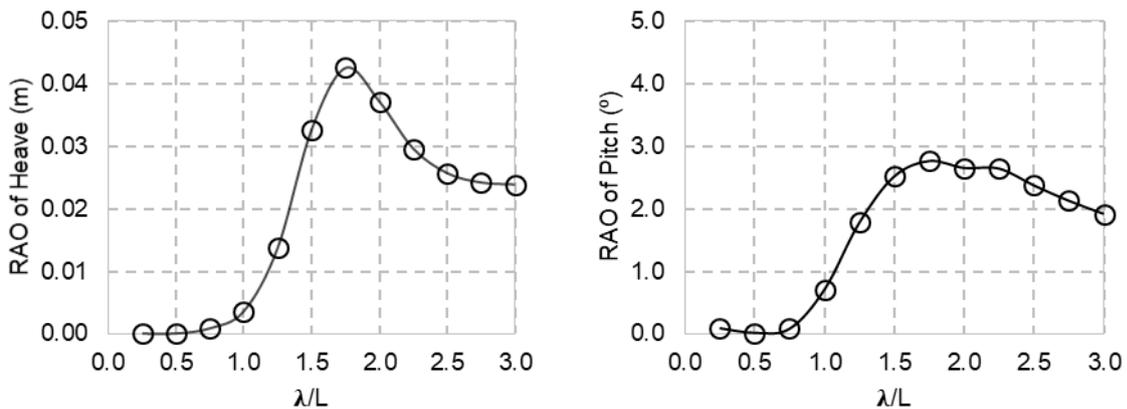

Figure 6. Heave and pitch motions for 'deep-V' catamaran ship at various wavelength, Fr = 0.8, Hw=/L=0.02586, Θ=0⁰.

Table 5. Heave and pitch motions of motions of 'deep-V' catamaran at various wavelength (λ/L)
Fr = 0.80, Hw/L = 0.0257 and Θ = 0°.

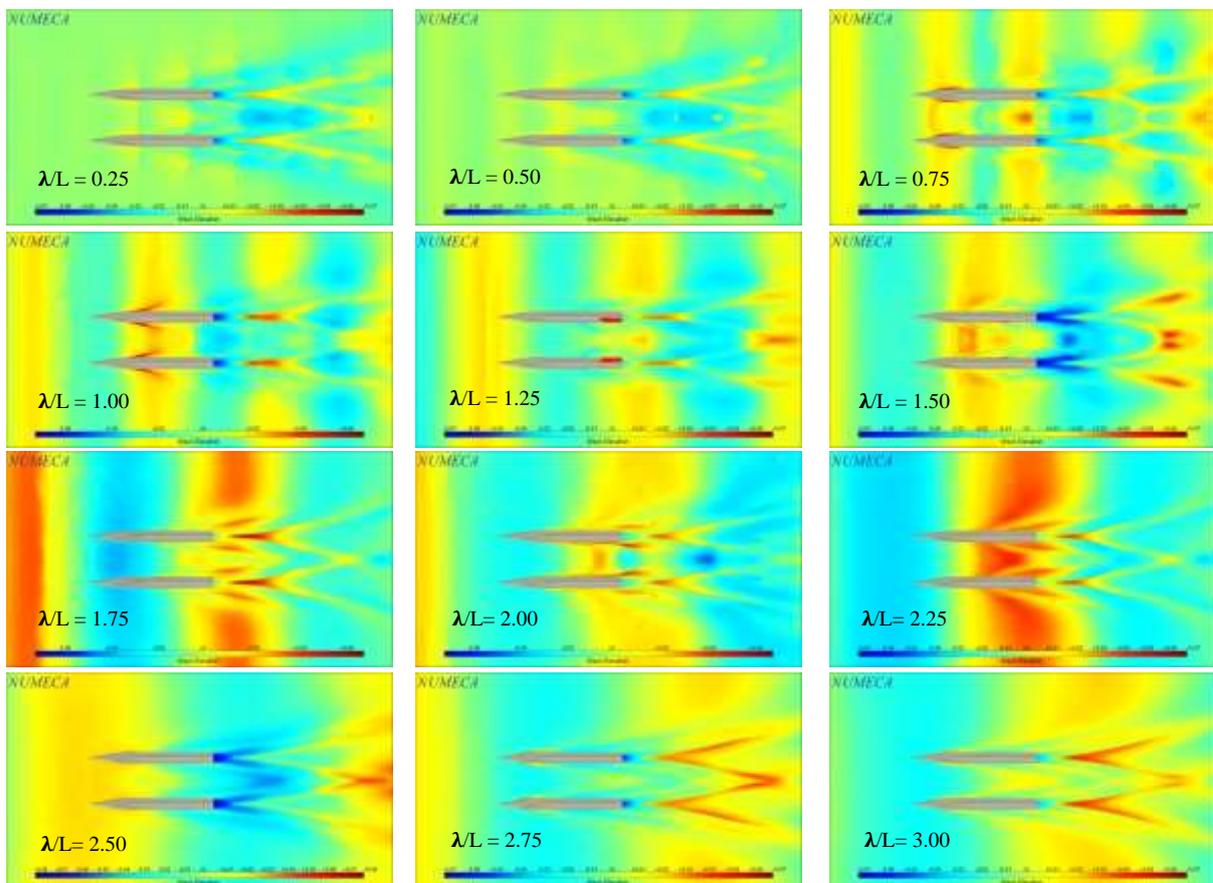| λ/ L	Fr = 0.80, Hw/L = 0.0257 and Θ = 0°	
	Heave Motion (m)	Pitch Motion (°)
0.25	0.000061	0.092110
0.50	0.000083	0.018732
0.75	0.000901	0.081824
1.00	0.003649	0.706973
1.25	0.013765	1.779765
1.50	0.032703	2.518655
1.75	0.042524	2.765494
2.00	0.037151	2.653424
2.25	0.029632	2.643677
2.50	0.025720	2.373719
2.75	0.024221	2.127916
3.00	0.023902	1.919303

Figure 7. Free surface elevation for 'deep-V' catamaran ship, Fr=0.8, Hw/L=0.02586, Θ=0°.

Effect of Wave height (Hw/L)

Referring to the Fig. 8, the prediction of RAO 'deep-V' catamaran response to wave height, Hw/L= 0.025 and 0.038 in the various wavelength from λ/L 0.25 up to 3.0. The result showed that the heave and pitch motion were obviously of similar trend with the result at Hw/L= 0.0257 and 0.0375. In case of Hw/L= 0.0375, the RAO for the heave and pitch motions of the 'deep-V' catamaran will generally result in higher responses as compared to Hw/L= 0.0257.

Besides that, looking into the range of wavelength (λ/L) 0.25 to 3.0, the 'deep-V' catamaran had small RAO of heave and pitch motions at λ/L=0.25 to 0.75. The RAO of heave and pitch motions increase in the range of λ/L=1.0 to 1.75 for both wave height. This situation can explained that, the increasing of ROA was prone to degrade the seakeeping performance due to the vigorous heave and pitch motion responses (Fitriadhy & Adam, 2017).

Table 6. Heave and pitch motions of motions of 'deep-V' catamaran at various wave height (Hw/L)
Fr = 0.80 and Θ = 0°

| λ/L	Fr = 0.80 and Θ = 0°			
	Hw/L = 0.0257		Hw/L = 0.0375	
	Heave Motion (m)	Pitch Motion (°)	Heave Motion (m)	Pitch Motion (°)
0.25	0.000061	0.092110	0.000244	0.036180
0.50	0.000083	0.018732	0.000279	0.063955
0.75	0.000901	0.081824	0.001855	0.288011
1.00	0.003649	0.706973	0.007857	1.138844
1.25	0.013765	1.779765	0.026942	3.235661
1.50	0.032703	2.518655	0.041236	3.888057
1.75	0.042524	2.765494	0.048213	4.133604
2.00	0.037151	2.653424	0.048232	4.017889
2.25	0.029632	2.643677	0.044126	3.851112
2.50	0.025720	2.373719	0.040508	3.623218
2.75	0.024221	2.127916	0.037038	3.233578
3.00	0.023902	1.919303	0.036148	2.907362
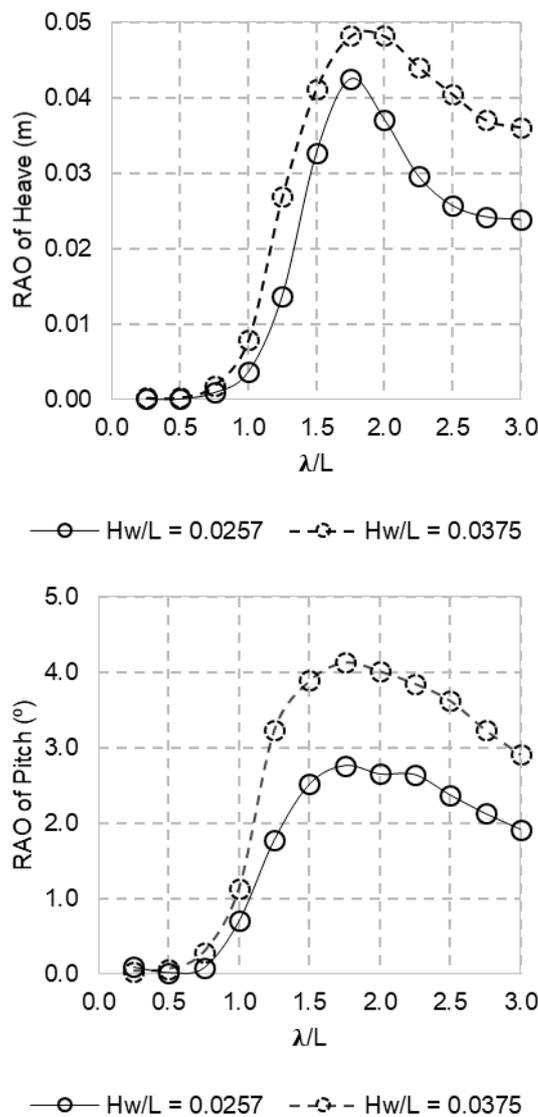
Figure 8. Heave and pitch motions for 'deep-V' catamaran ship at various wave height, Fr = 0.8 and Θ=0°.

CONCLUSIONS

This preliminary investigation using computational simulation on 'deep-V' catamaran showed that the results are presented in the form of response amplitude operator for both heave and pitch motions and described the seakeeping performance. The effect of various Froude number (Fr), wavelength (λ/L) and wave-height (Hw/L) can be drawn as follow:

i) The increase of Froude number up to 1.25 was inversely proportional with the RAO of the heave and pitch motions, where this condition was prone to improve the seakeeping performance of the 'deep-V' catamaran.

ii) It was noted here that the maximum RAO of heave and pitch motions of the 'deep-V' catamaran occurred at λ/L=1.75. However, the further increase wavelength from λ/L 1.75 to 3.0 showed that the RAO of the heave and pitch motions decrease that lead to be better seakeeping performance.

iii) The increase wave-height from 0.0257 to 0.0375 was proportional to the RAO of the heave and pitch motions that resulted in a lower seakeeping ability.

In general, the effect of Froude number, wavelength and wave-height was showed in increase and decrease the value of heave and pitch motions lead to the downgrade and better seakeeping performance respectively. The seakeeping performance also presented in the form of high and lower Response Amplitude Operator.

ACKNOWLEDGMENT

REFERENCES

Abdul Ghani, P., & Wilson, P. (2017). Experimental analysis of the seakeeping performance of catamaran forms with bulbous bows. *International Shipbuilding Progress (Preprint)*, *65*(1), 1-28. http://dx.doi.org/10.3233/ISP-170140 .

Aribenchi, V. (2017). *Dynamics of Asymmetrical Configurations of Catamaran Hull Forms*. Thesis. Florida Institute of Technology. USA.

Belknap, W. F. (2008). *A computationally efficient method for nonlinear multihull seakeeping*. Thesis. University of Michigan. USA.

Castiglione, T., & Bova, S. Hydrodynamic Analysis of a Catamaran in Calm Water and in Waves. *Conference Paper*.

Fitriadhy, A., & Adam, N. A. (2017). Heave and pitch motions performance of a monotricat ship in head-seas. *International Journal of Automotive and Mechanical Engineering*, *14*, 4243-4258. http://dx.doi.org/10.15282/ijame.14.2.2017.10.0339.

Fitriadhy, A., Razali, N., & AqilahMansor, N. (2017). Seakeeping performance of a rounded hull catamaran in waves using CFD approach. Journal of Mechanical Engineering and Sciences, *11*(2), 2601-2614. http://dx.doi.org/10.15282/jmes.11.2.2017.4.0238

Grande, K., & Xia, J. (2002). Prediction of slamming occurrence on catamaran cross structures. *ASME 2002 21st International Conference on Offshore Mechanics and Arctic Engineering,* 525-533. http://dx.doi.org/10.1115/OMAE2002-28344

Gunawan, Y., Kurniawan, T., & Jamaluddin, A. (2015). Experimental Study Resistances of Asymmetrical Pentamaran Model with Separation and Staggered Hull Variation of Inner Side-Hulls. *Internatonal Journal of Fluid Mechanical Research*, *42*(1), 820-94. http://dx.doi.org/10.1615/InterJFluidMechRes.v42.i1.60.

Haase, M., Zurcher, K., Davidson, G., Binns, J. R., Thomas, G., & Bose, N. (2016). Novel CFD-based full-scale resistance prediction for large medium-speed catamarans. *Ocean Engineering*, *111*(1), 198-208. http://dx.doi.org/10.1016/j.oceaneng.2015.10.018

Iglesias, A. S., Zamora, R., Fernández, D., & Pavón, C. L. (2006). Catamaran wave resistance and central wave cuts for CFD validation. In: Maritime Transportation and Exploitation of Ocean and Coastal Resources: *Proceedings of the 11th International Congress of the International Maritime Association of the Mediterranean*, Lisbon, Portugal. http://dx.doi.org/10.1201/9781439833728.ch18

Lin, C.-T., Lin, T.-Y., Lin, C.-W., Hsieh, Y.-W., Lu, L., & Hsin, C.-Y. (2017). Investigation of the Seakeeping Performance of Twin Hull Vessels by Different Computational Methods. *10th International Workshop on Ship and Marine Hydrodynamics*, Keelung, Taiwan. 1-10.

Luhulima, R. B., Setyawan, D., & Utama, I. (2014). Selecting monohull, catamaran and trimaran as suitable passenger vessels based on stability and seakeeping criteria. *The 14th International Ship Stability Workshop (ISSW)*, Kuala Lumpur, Malaysia. 262-266.

Salas, M., Luco, R., Sahoo, P., Browne, N., & Lopez, M. (2004). Experimental and CFD

resistance calculation of a small fast catamaran. *The 4th International Conference on High Performance Marine Vehicles.* 1-7.

Setyawan, D., Utama, I. K., Murdijanto, M., Sugiarso, A., & Jamaluddin, A. (2010). Development of catamaran fishing vessel. *IPTEK The Journal for Technology and Science*, *21*(4). http://dx.doi.org/10.12962/j20882033.v21i4.90

Sun, H., Jing, F., Jiang, Y., Zou, J., Zhuang, J., & Ma, W. (2016). Motion prediction of catamaran with a semisubmersible bow in wave. *Polish Maritime Research*, *23*(1), 37-44. http://dx.doi.org/10.1515/pomr-2016-0006

Swidan, A. (2016). *Catamaran wetdeck slamming: a numerical and experimental investigation.* Thesis. University of Tasmania,

Vakilabadi, K. A., Khedmati, M. R., & Seif, M. S. (2014). Experimental study on heave and pitch motion characteristics of a wave-piercing trimaran. *Transactions of FAMENA*, *38*(3), 13-26.

Yanuar, Ibadurrahman, Karim, S., & Ichsan, M. (2017). Experimental study of the interference resistance of pentamaran asymmetric side-hull configurations. *The AIP Conference Proceedings. 1826*(1). http://dx.doi.org/10.1063/1.4979241.

Zotti, I. (2007). Medium speed catamaran with large central bulbs: experimental investigation on resistance and vertical motions. *International Conference on Marine Research and Transportation ICMRT'07*, Naples, Italy. 167-174.